

# Spectral interferometric polarised coherent anti-Stokes Raman spectroscopy

Brad Littleton,<sup>1,\*</sup> Thomas Kavanagh,<sup>1</sup> Frederic Festy,<sup>2</sup> and David Richards<sup>1,†</sup>

<sup>1</sup>*Department of Physics, King's College London, Strand, London, WC2R 2LS*

<sup>2</sup>*Biomaterials, Biomimetics and Biophotonics Department,  
King's College London Dental Institute, Floor 17 Tower Wing,  
Guy's Hospital, London Bridge, London SE1 9RT, UK*

We have developed an interferometric implementation of coherent anti-Stokes Raman scattering (CARS) which enables broadband coherent Raman spectroscopy free from non-resonant background (NRB), with a signal strength proportional to concentration. Spectra encode mode symmetry information into the amplitude response which can be directly compared to polarised spontaneous Raman spectra. The method requires only passive polarisation optics and is suitable for a wide range of laser linewidths and pulse durations.

Spontaneous Raman scattering provides a powerful optical route to obtain chemically specific information. Its application to microscopy enables imaging using molecular vibrations as a contrast mechanism and mapping of cell and tissue constituents based on their chemical signature [1, 2]. Coherent Raman scattering (CRS) is the non-linear multiphoton equivalent and allows much faster acquisition, [3, 4] with intrinsic optical sectioning in imaging [5]. However, while CRS imaging has been very successfully employed for imaging individual Raman bands, it struggles to harness the powerful chemical specificity provided by spectral detection in the Raman fingerprint region. In particular, quantitative broadband coherent Raman spectroscopy of biological samples, analogous to spontaneous Raman spectroscopy, has proven difficult to achieve primarily due to the coherent backgrounds inherent to CRS. In this letter we report on a new method for quantitative broadband CRS spectral imaging, which uses passive polarisation optics combined with spectrally-resolved balanced homodyne detection. The technique has relaxed requirements on spectral phase and instrument stability and provides full access to the Raman fingerprint region, while retaining the advantages of enhanced signal and optical sectioning inherent to CRS.

The two most widely used CRS techniques are stimulated Raman scattering (SRS) and CARS (Fig 1(a)) [6]. At intensities suitable for biological samples, SRS requires heterodyne methods [7, 8] to detect the signal against the coherent background of the excitation fields; such methods require wavelength scanning to build up spectral information. CARS is a four wave mixing (FWM) process with a signal field generated at the anti-Stokes frequency  $\omega_{aS} = \omega_{pr} + \omega_p - \omega_S$  which is spectrally separated from the excitation fields ( $\omega_p, \omega_S, \omega_{pr}$  are denoted the pump, Stokes and probe fields, respectively). CARS can therefore simultaneously generate an entire vibrational spectrum by using a spectrally broad Stokes beam [9], making CARS suitable for rapid detection of vibrational spectra, particularly in microscopy.

The coherent background in CARS arises from FWM processes that are independent of vibrational transitions (Fig 1(a)). The anti-Stokes intensity is determined by the

third order susceptibility, which (away from electronic resonances) is given by

$$|\chi|^2 = \chi_{NR}^2 + 2\chi_{NR} \text{Re}\{\chi_R\} + |\chi_R|^2, \quad (1)$$

where  $\chi_R$  and  $\chi_{NR}$  are components resonant and non-resonant with vibrational modes, respectively. Since  $\chi_R$  is proportional to the number of resonant modes in a medium, the concentration dependence of CARS is quadratic and non-linearly mixed with the non-resonant background (NRB). The interferometric (second) term, however, is linear in  $\chi_R$  and is amplified by  $\chi_{NR}$ .  $\text{Re}\{\chi_R\}$  is dispersive and antisymmetric about the vibrational line-centre; however,  $\text{Im}\{\chi_R\}$  is directly related to the spontaneous Raman spectrum [6].

Many methods have been developed to remove the effect of the NRB from CARS spectra [10]. Non-interferometric techniques, such as polarisation-based [11–13] and time-resolved methods [14, 15], recover a (typically small) proportion of the energy in the third term of (1). However, the interferometric term is the largest source of signal for weak resonances and, below the damage threshold of biological samples, CRS has been shown to be faster than spontaneous Raman spectroscopy only if this term is detected [4, 16].

$\text{Im}\{\chi_R\}$  may be recovered through interference between the anti-Stokes field and a local oscillator (LO), which may be generated either externally [17–20], or by using the NRB as an internal LO [21–23]. Broadband external approaches acquire an entire spectrum simultaneously via spectral interferometry, requiring high stability [24] and broadband transform limited laser sources [25] (precluding the use of fields generated in photonic crystal fibres (PCF), which are typically much broader). Using the NRB as the LO ensures that the phase relationship between the LO and anti-Stokes fields is fixed, which relaxes stability and spectral coherence requirements; however, as the LO is in phase with  $\text{Re}\{\chi\}$ , recovering  $\text{Im}\{\chi\}$  is not trivial. Previous experimental implementations also need broad transform limited pulses [22, 23, 26–28], or require phase scanning [21, 28].

Computational internal LO approaches have also been developed, which use the  $\chi_{NR} \text{Re}\{\chi_R\}$  term present in

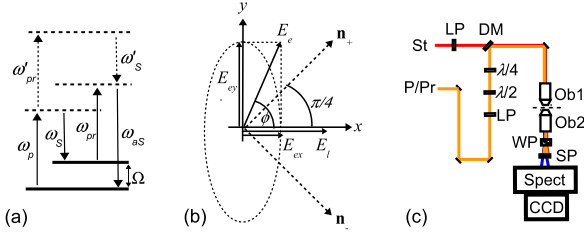


Figure 1: (colour online) (a) Energy level diagram. CARS involves the path  $\omega_p \rightarrow \omega_S \rightarrow \omega_{pr} \rightarrow \omega_{aS}$ , SRS is  $\omega_p \rightarrow \omega_S \rightarrow \Omega$  (where  $\Omega$  is a vibrational resonance). An example non-resonant FWM pathway is shown as  $\omega_p \rightarrow \omega'_{pr} \rightarrow \omega'_S \rightarrow \omega_{aS}$ . (b) Polarisations for SIP-CARS with one elliptical (or circular) polarised field  $E_e$  and one linear field  $E_l$ . Detection is performed along  $\hat{n}_+$  and  $\hat{n}_-$ .  $E_e$  is shown as the input to a  $\lambda/4$  plate (orientated at angle  $\phi$  to the fast axis) to generate the desired elliptical polarisation. For a circular Stokes/linear pump:  $E_e = E_S$ ,  $E_l = E_p = E_{pr}$ ,  $\phi = \pi/4$ . For elliptical pump/linear Stokes:  $E_e = E_p = E_{pr}$ ,  $E_l = E_S$ ,  $\phi = \pi/8$  or  $3\pi/8$ . (c) Experimental setup. Both pump/probe (P/Pr: 1050 nm) and Stokes (St: 1070-1600 nm) beams were derived from a commercial supercontinuum source with two outputs (repetition rate 20MHz,  $\sim 5$ ps pulses at the sample). Beams were combined on a dichroic mirror (DM) and focussed into the sample by a 1.3NA oil immersion DIC objective lens (Ob1), where the power of each beam was 30 mW. Samples were prepared between two coverslips, separated by  $< 60 \mu\text{m}$ . The signal was collected by a 0.75NA air objective (Ob2), separated from the excitation fields by a shortpass filter (SP), and then dispersed via grating spectrometer onto a deep depletion CCD. The pump/probe ellipticity was controlled by a combination of linear polariser (LP) and zero-order half- and quarter-waveplates ( $\lambda/2$  and  $\lambda/4$ , respectively). A Wollaston prism (WP) was placed after Ob2 to separate the two detection polarisations on the CCD. The beams were again circularly polarised before the spectrometer by an achromatic quarter-wave plate (not shown) to account for the different grating reflectivity for each polarisation.

raw CARS spectra to calculate  $\text{Im}\{\chi_R\}$  [29, 30]. These produce good approximations to  $\text{Im}\{\chi_R\}$  if the spectra are of sufficient width, however both methods intrinsically produce a spectrally varying error signal, which increases at resonances (up to 10%)[31]. Both techniques also require prior or post estimation of the spectral variation of the NRB (effectively the spectral variation of the Stokes field) from a reference material, which is often compromised by the presence of a residual resonant response. Changes of the background spectrum during an acquisition leads to errors that can mask the weaker resonances in the fingerprint region of biological samples[4].

We describe here a new internal LO technique, Spectral Interferometric Polarised CARS (SIP-CARS), that is significantly simpler to implement than previous experimental approaches. It does not have stringent requirements on the lasers used, and is suitable for narrowband, multiline and broadband systems. Transform limited pulses are not required and PCF generated supercontinua can

therefore be used to generate broad, NRB-free, vibrational spectra. Furthermore, the NRB is removed without requiring an independent measurement of its spectral variation. The technique is similar to Dual Quadrature Spectral Interferometry (DQSI)[22, 24, 28, 32], except that the fields have different frequencies and hence only interfere via the non-linear response. As a result, the two quadratures measured in SIP-CARS (i.e. the real and imaginary components of the non-linear response) contain different linear combinations of the tensor elements of  $\chi$ , due to polarisation mixing. The third-order response is solved exactly, without assumptions on the relative strength of resonant and non-resonant components[22, 33].

To illustrate the method, consider CARS with a (right-hand) circularly polarised Stokes, and pump and probe linearly polarised along the  $x$ -axis, as in Figure 1(b). For convenience, we express the Stokes electric field in terms of the equivalent linear polarisation,  $E_S$ , used to generate it via a  $\lambda/4$  plate; so, the field along  $x$ - and  $y$ -axes is  $E_{S_x} = E_S/\sqrt{2}$  and  $E_{S_y} = iE_S/\sqrt{2}$  (along any two orthogonal directions the Stokes electric field will differ in phase by  $\pi/2$ ). The susceptibility can be separated into diagonal (e.g.  $\chi_{iiii}$ ) and off-diagonal (e.g.  $\chi_{ijij}$ ) elements; the off-diagonal terms mediate the coupling of orthogonally polarised excitations into the detected polarisation. Considering the polarisation,  $P_+$ , induced in the medium along the  $\hat{n}_+$  axis, at  $+\pi/4$  to the pump and probe polarisation, we have

$$P_+ = \frac{1}{2}\chi_{1111}E_{pr}E_p(E_S^+)^* + \frac{1}{2}\chi_{1221}E_{pr}E_p(E_S^+)^* + \frac{1}{2}\chi_{1122}E_{pr}E_p(E_S^-)^* + \frac{1}{2}\chi_{1212}E_{pr}E_p(E_S^-)^*$$

where  $E_p$  and  $E_{pr}$  are the electric fields of the pump and probe, and  $E_S^+$  and  $E_S^-$  are the components of the Stokes along  $\hat{n}_+$  and  $\hat{n}_-$ , respectively (Fig. 1(b)). As  $E_S^+ = iE_S^-$ , the last two terms lag the first two in phase by  $\pi/2$ . Imaginary components of the last two terms therefore interfere with real components of the first two, with the strength of the interference determined by the relative strength of the diagonal and off-diagonal tensor elements. Similarly, for  $P_-$  the  $E_S^+$  and  $E_S^-$  terms are swapped, and the last two terms lead the first two by  $\pi/2$ . Imaginary components are therefore added to the real components along  $\hat{n}_+$ , and subtracted from them along  $\hat{n}_-$ ; spectral interferometric detection is performed by taking the difference between spectra measured at these polarisations, leaving the purely imaginary components [22].

The induced polarisations are more succinctly expressed within a basis including the pump and probe polarisations,

$$\begin{aligned} P_x &= \frac{1}{\sqrt{2}}\chi_{1111}E_{pr}E_pE_S^* \\ P_y &= -\frac{i}{\sqrt{2}}\chi_{2112}E_{pr}E_pE_S^* \end{aligned} \quad (2)$$

Along the detection axes  $\hat{n}_+$  and  $\hat{n}_-$  the induced polarisations are  $P_+ = \frac{1}{\sqrt{2}}(P_x + P_y)$  and  $P_- = \frac{1}{\sqrt{2}}(P_x - P_y)$ , and the anti-Stokes signals are  $S_+ \propto P_+ P_+^*$ ,  $S_- \propto P_- P_-^*$ . The sum and difference of the anti-Stokes intensities are then  $\Sigma S = S_+ + S_- \propto P_x P_x^* + P_y P_y^*$  and  $\Delta S = S_+ - S_- \propto P_x P_y^* + (P_x P_y^*)^*$ , respectively. The difference signal is therefore given by

$$\Delta S \propto \text{Im} \{ \chi_{1111} \chi_{2112}^* \} I_{pr} I_p I_S \quad (3)$$

where  $I_i = E_i E_i^*$  are the beam intensities. Separating the susceptibilities into resonant and nonresonant components  $\chi_{ijkl} = \chi_{ijkl}^{NR} + \chi_{ijkl}^R$ , assuming an isotropic medium ( $\chi_{2112} = \chi_{1221}$ ,  $\chi_{1111} = \chi_{1212} + \chi_{1221} + \chi_{1122}$ ), and noting that the non-resonant terms possess Kleinman symmetry[34] ( $\chi_{1111}^{NR} = \chi_{NR}$ ,  $\chi_{1212}^{NR} = \chi_{1122}^{NR} = \chi_{1221}^{NR} = \chi_{NR}/3$ ) this becomes

$$\begin{aligned} \Delta S \propto \chi_{NR} \text{Im} \{ \chi_{1111}^R - 3\chi_{1221}^R \} I_{pr} I_p I_S \\ \propto (1 - 3\rho) \chi_{NR} \text{Im} \{ \chi_{1111}^R \} I_{pr} I_p I_S \end{aligned} \quad (4)$$

where  $\rho = \chi_{1221}^R / \chi_{1111}^R$  is the CARS depolarisation ratio of the resonance [35]. The difference spectrum is therefore linear in the imaginary component of  $\chi$ , is amplified by  $\chi_{NR}$ , and contains no real, dispersive terms or non-resonant contributions. Due to the linear response, well established linear multivariate analyses such as principal component analysis can be applied. Mode symmetry information is mixed into the amplitude response through the depolarisation ratio,  $\rho$  ( $0 < \rho < 3/4$ ), and the spectrum can be compared directly to polarised spontaneous Raman spectra.

Because the interference is effectively between  $\pi/2$  phase shifted copies of the same fields there are no extra requirements on the coherence of the excitation pulses. Moreover, if spectra are measured simultaneously, incoherent backgrounds (such as two-photon fluorescence) and any variation of the real components of the CARS signal are common-mode in  $S_+$  and  $S_-$  and are automatically subtracted out (though they will still contribute shot noise to the difference spectrum). This is essentially a balanced homodyne detection scheme, except that in this case the signal arises in the low noise difference channel rather than the sum channel.

At the focus of a high NA lens it is easier to control the circular polarisation of a narrowband beam rather than a broadband one, and, commonly, the pump and probe fields are supplied by the same beam, so  $E_{pr} = E_p$ . To address this we can generalise (4) to the case of arbitrary ellipticity of both Stokes and pump beams [38]

$$\Delta S \propto C(\theta, \phi) I_p^2 I_S (1 - 3\rho) \chi_{NR} \text{Im} \{ \chi_{1111}^R \} \quad (5)$$

where

$$C(\theta, \phi) = \frac{1}{2} [\sin(4\phi) + \sin(2\theta) + \sin(2\theta) \cos(4\phi)]. \quad (6)$$

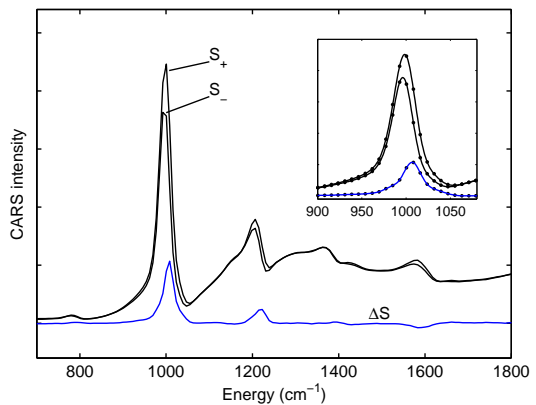


Figure 2: (colour online) Interferometric correction of the NRB in toluene.  $S_+$  and  $S_-$  are the raw CARS spectra measured along the  $\hat{n}_+$  and  $\hat{n}_-$  directions of Fig. 1(b). The difference spectrum  $\Delta S = S_+ - S_-$  contains non-dispersive lineshapes at the correct Raman shifts (c.f. Fig. 3). Inset: close-up of the region around  $1000 \text{ cm}^{-1}$  showing the  $\Delta S$  peak shifted with respect to the dispersive CARS peaks (lines are a guide to the eye).

$\theta$  and  $\phi$  characterise the ellipticity of the Stokes and pump/probe fields, respectively, and are defined as the angle between the fast axis (set parallel to the  $x$ -axis) of a quarter waveplate and an input linear polarisation. For the experimentally practical situation where the broadband Stokes is constrained to be linear (ie  $C(0, \phi)$ ) the SIP-CARS signal,  $\Delta S$ , is maximised for an elliptical pump with  $\phi = \pi/8, 3\pi/8$ . Significantly,  $\Delta S$  retains the same spectral form regardless of the ellipticity of the excitation beams. In general, the NRB will be removed as long as the polarisation ellipses are symmetric with respect to the measurement axes, while the ellipticity determines the amplitude of  $\Delta S$ . This decoupling of NRB removal and signal amplitude simplifies the alignment under tight focussing conditions. Requirements on polarisation purity are somewhat relaxed and the polarisation can be set *in situ* at the focus by iteratively minimising the NRB and maximising the difference signal at resonance.

Experiments with an elliptical pump and broadband linear Stokes were performed with the apparatus detailed in Figure 1(c). Dispersion in the long internal PCF of the source limited temporal overlap between pump/probe and Stokes, such that the effective Stokes range was  $750\text{--}2300 \text{ cm}^{-1}$  (though strong resonances were detectable to  $3000 \text{ cm}^{-1}$  [39]). The pump/probe width was  $30 \text{ cm}^{-1}$ . This system served as a rigorous demonstration of the robustness of the technique, as the PCF generated Stokes beam has relatively low spectral coherence, and all the wavelengths used were outside the design range for the input objective lens which significantly affected SNR through poor focussing performance. Single-shot broadband interferometric NRB removal for this system

would not be possible by any other optical technique.

Correction of Raman lineshapes and removal of the NRB in SIP-CARS is shown for toluene in Figure 2. The two CARS spectra,  $S_+$  and  $S_-$ , measured at  $\pm 45^\circ$  from the Stokes polarisation exhibit the asymmetric dispersive lineshapes and spectrally varying NRB (the variation reflecting the spectrum of the Stokes beam) which is characteristic of CARS measurements. The difference spectrum,  $\Delta S$ , shows no NRB and Raman peaks are symmetric and occur at the correct vibrational energy. The inset shows this in greater detail for the ring breathing mode at  $1004 \text{ cm}^{-1}$  [36].

Direct comparison to spontaneous Raman spectra can be made by equating the depolarisation ratio in Equation 4 with the spontaneous Raman depolarisation ratio [35, 37]  $\rho = R_\perp/R_\parallel$ , where  $R_\parallel$  and  $R_\perp$  are spontaneous Raman spectra with incident and scattered polarisation mutually parallel and perpendicular, respectively. Then  $R_\parallel \propto \text{Im}\{\chi_{1111}\}$  and  $R_\perp \propto \text{Im}\{\chi_{1221}\}$ , and from Equation 4,

$$\frac{\Delta S}{I_S} \propto R_\parallel - 3R_\perp. \quad (7)$$

Note that the normalisation of the difference spectrum by  $I_S$  corrects the peak amplitudes for variation in the Stokes spectrum to allow comparison with the spontaneous Raman spectrum; it is not necessary for removing the NRB or for quantitative measurements. For a non-resonant sample,  $\chi_{1111} = \chi_{NR}$  and  $\chi_{1221} = \chi_{NR}/3$ , so (2) reduces to  $P_x = \chi_{NR}E_p^2E_S^*/\sqrt{2}$ ,  $P_y = -i\chi_{NR}E_p^2E_S^*/3\sqrt{2}$  (where we have set  $E_{pr} = E_p$ ). The sum spectrum,  $\Sigma S$ , is then

$$\Sigma S \propto P_x P_x^* + P_y P_y^* = \frac{5}{9} I_p^2 I_S \chi_{NR}^2. \quad (8)$$

The spectral form of  $I_S$  can therefore be determined from that of  $\Sigma S$  obtained from a non-resonant medium; we have employed a glass coverslip for this purpose as the glass resonant response is slowly varying and weakens towards higher wavenumbers. We find complete agreement between SIP-CARS and spontaneous Raman in terms of both spectral position and relative peak heights (shown for cyclohexane and toluene in Figure 3). As expected from (5), the amplitude of each Raman line is scaled by the depolarisation ratio, with peaks going negative for resonances with  $\rho > 1/3$ , providing a powerful approach for the differentiation of otherwise similar spectra on the basis of mode symmetry. Modes for which  $\rho \simeq 1/3$  do not appear, such as the  $\text{CH}_3$  'umbrella' deformation mode of toluene at  $1379 \text{ cm}^{-1}$ .

As the non-resonant response,  $\chi_{NR}$ , amplifies the resonant CARS signal, quantitative measurements in heterogeneous media require account to be taken of any variation of  $\chi_{NR}$ ; for example, as density changes across a sample. SIP-CARS is self-calibrating, in that  $\chi_{NR}$  can be

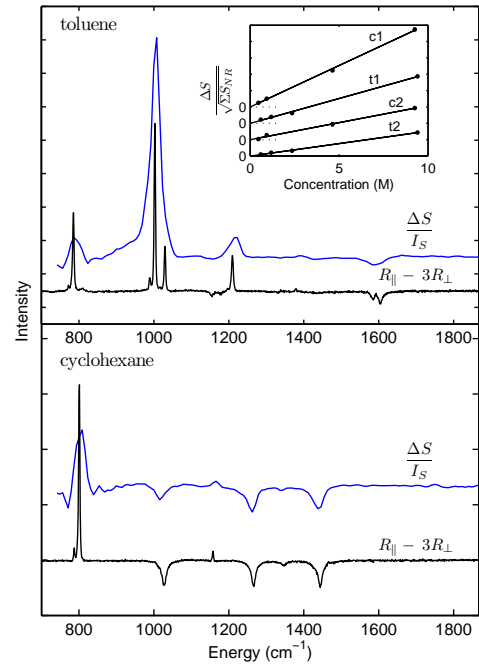


Figure 3: (colour online) Comparison of normalised SIP-CARS to the spontaneous Raman spectrum formed by  $R_\parallel - 3R_\perp$  ( $R_\parallel$  parallel polarised,  $R_\perp$  perpendicular polarised). Curves offset for clarity. Top panel: cyclohexane. Bottom panel: toluene. The SIP-CARS and spontaneous Raman spectra agree closely, to within the resolution of the SIP-CARS measurement. Inset: Concentration dependence of various resonances of toluene (in methanol: 100% to 6.25% toluene) and cyclohexane (in toluene: 100% to 5% cyclohexane) in the presence of strongly varying NRB (see text).  $\Sigma S_{NR}$  is  $\Sigma S$  integrated over the range  $1800\text{--}1980 \text{ cm}^{-1}$ . Error bars are within marker size. Curves have been offset and scaled for clarity (toluene: t1= $1004 \text{ cm}^{-1}$ , t2= $1208 \text{ cm}^{-1}$ ; cyclohexane: c1= $1267 \text{ cm}^{-1}$ , c2:  $1444 \text{ cm}^{-1}$ ).

monitored in the same measurement if a spectrum contains a non-resonant region (such as the 'quiet' region exhibited by biological samples). From (8), measuring  $\Sigma S$  at a reference frequency away from resonances gives a quantity  $\Sigma S_{NR} \propto \chi_{NR}^2$ . The SIP-CARS difference spectrum can therefore be normalised by  $\sqrt{\Sigma S_{NR}}$  to give a signal which is linear in concentration and independent of the strength of the non-resonant response.

We find that the NRB signal from toluene is approximately twice as strong as for cyclohexane and much stronger than for methanol. Therefore, to demonstrate linear concentration dependence in a situation with varying NRB, a range of mixtures of cyclohexane in toluene and toluene in methanol were investigated. For cyclohexane in toluene the NRB therefore increased with decreasing cyclohexane concentration, while for toluene in methanol the NRB had the opposite trend.  $\Sigma S_{NR}$  was measured by integrating the sum spectrum over the range  $1800\text{--}1980 \text{ cm}^{-1}$ , and used to normalise the SIP-CARS measurement, which displayed a linear signal dependence

on concentration (inset of Figure 3).

In summary, by exploiting the third-order polarisation response, SIP-CARS allows acquisition of CRS spectra free of NRB, with complete agreement to spontaneous Raman measurements. Spectra are amplified by the non-resonant response and are quantitative, with a linear concentration dependence. The method uses only passive polarisation optics, has low stability requirements, and is suitable for any laser system capable of generating CARS, permitting single-shot interferometric NRB removal with broad PCF generated supercontinua.

This work was supported by the Biotechnology and Biological Sciences Research Council (BB/F016344) and the European Metrology Research Programme (NEW02-REG2).

---

\* Electronic address: bradley.littleton@kcl.ac.uk

† Electronic address: david.r.richards@kcl.ac.uk

- [1] S. Stewart, R. J. Priore, M. P. Nelson, and P. J. Treado, *Annual Review of Analytical Chemistry* **5**, 337 (2012), pMID: 22524218, <http://www.annualreviews.org/doi/pdf/10.1146/annurev-anchem-062011-143152>, URL <http://www.annualreviews.org/doi/abs/10.1146/annurev-anchem-062011-143152>.
- [2] G. J. Puppels, F. F. M. de Mul, C. Otto, J. Greve, M. Robert-Nicoud, D. J. Arndt-Jovin, and T. M. Jovin, *Nature* **347**, 301 (1990), URL <http://dx.doi.org/10.1038/347301a0>.
- [3] B. G. Saar, C. W. Freudiger, J. Reichman, C. M. Stanley, G. R. Holtom, and X. S. Xie, *Science* **330**, 1368 (2010), URL <http://www.sciencemag.org/content/330/6009/1368>.
- [4] S. H. Parekh, Y. J. Lee, K. A. Aamer, and M. T. Cicerone, *Biophysical Journal* **99**, 2695 (2010).
- [5] X. J. Cheng and X. S. Xie, *J Phys Chem B* **108**, 827 (2004).
- [6] G. L. Eesley, *Coherent Raman Spectroscopy*, vol. 9 (Pergamon Press New York, 1981).
- [7] C. W. Freudiger, W. Min, B. G. Saar, S. Lu, G. R. Holtom, C. He, J. C. Tsai, J. X. Kang, and X. S. Xie, *Science* **322**, 1857 (2008), URL <http://www.sciencemag.org/cgi/content/abstract/322/5908/1857>.
- [8] M. N. Slipchenko, R. A. Oglesbee, D. Zhang, W. Wu, and J.-X. Cheng, *Journal of Biophotonics* **5**, 801 (2012).
- [9] H. Kano and H. Hamaguchi, *Applied Physics Letters* **86** (2005), ISSN 0003-6951.
- [10] J. P. R. Day, K. F. Domke, G. Rago, H. Kano, H.-o. Hamaguchi, E. M. Vartiainen, and M. Bonn, *The Journal of Physical Chemistry B* **115**, 7713 (2011), <http://pubs.acs.org/doi/pdf/10.1021/jp200606e>, URL <http://pubs.acs.org/doi/abs/10.1021/jp200606e>.
- [11] S. A. Akhmanov, A. F. Bunkin, S. G. Ivanov, and N. I. Koroteev, *JETP Letters* **25**, 416 (1977).
- [12] J.-L. Oudar, R. W. Smith, and Y. R. Shen, *Applied Physics Letters* **34**, 758 (1979), URL <http://link.aip.org/link/?APL/34/758/1>.
- [13] F. Lu, W. Zheng, and Z. Huang, *Optics Letters* **33**, 2842 (2008).
- [14] A. Volkmer, L. D. Book, and X. S. Xie, *Applied Physics Letters* **80**, 1505 (2002).
- [15] Y. J. Lee and M. T. Cicerone, *Appl. Phys. Lett.* **92**, 041108 (2008), URL <http://link.aip.org/link/?APL/92/041108/1>.
- [16] M. Cui, B. R. Bachler, and J. P. Ogilvie, *Opt. Lett.* **34**, 773 (2009), URL <http://ol.osa.org/abstract.cfm?URI=ol-34-6-773>.
- [17] E. O. Potma, C. L. Evans, and X. S. Xie, *Optics Letters* **31**, 241 (2006).
- [18] C. Muller, T. Buckup, B. von Vacano, and M. Motzkus, *Journal of Raman Spectroscopy* **40**, 809 (2009).
- [19] M. Jurna, J. P. Korterik, C. Otto, J. L. Herek, and H. L. Offerhaus, *Optics Express* **16**, 15863 (2008), ISSN 1094-4087.
- [20] K. Orsel, E. T. Garbacik, M. Jurna, J. P. Korterik, C. Otto, J. L. Herek, and H. L. Offerhaus, *Journal of Raman Spectroscopy* **41**, 1678 (2010), ISSN 1097-4555, URL <http://dx.doi.org/10.1002/jrs.2621>.
- [21] T. W. Kee, H. Zhao, and M. T. Cicerone, *Opt. Express* **14**, 3631 (2006), URL <http://www.opticsexpress.org/abstract.cfm?URI=oe-14-8-3631>.
- [22] S.-H. Lim, A. G. Caster, and S. R. Leone, *Phys. Rev. A* **72**, 041803 (2005), URL <http://link.aps.org/abstract/PRA/v72/e041803>.
- [23] D. Oron, N. Dudovich, and Y. Silberberg, *Phys. Rev. Lett.* **90**, 213902 (2003), URL <http://link.aps.org/abstract/PRL/v90/e213902>.
- [24] C. L. Evans, E. O. Potma, and X. S. N. Xie, *Optics Letters* **29**, 12923 (2004).
- [25] P. D. Chowdary, W. A. Benalcazar, Z. Jiang, D. M. Marks, S. A. Boppart, and M. Gruebele, *Analytical Chemistry* **82**, 3812 (2010).
- [26] J. Sung, B.-C. Chen, and S.-H. Lim, *Journal of Raman Spectroscopy* **42**, 130 (2011), ISSN 1097-4555, URL <http://dx.doi.org/10.1002/jrs.2647>.
- [27] D. Oron, N. Dudovich, and Y. Silberberg, *Phys. Rev. Lett.* **89**, 273001 (2002), URL <http://link.aps.org/doi/10.1103/PhysRevLett.89.273001>.
- [28] A. Wipfler, J. Rehbinder, T. Buckup, and M. Motzkus, *Optics Letters* **37** (2012), URL <http://www.opticsexpress.org/abstract.cfm?URI=oe-14-8-3631>.
- [29] E. M. Vartiainen, H. A. Rinia, M. Muller, and M. Bonn, *Optics Express* **14**, 3622 (2006).
- [30] Y. Liu, Y. J. Lee, and M. T. Cicerone, *Opt. Lett.* **34**, 1363 (2009), URL <http://ol.osa.org/abstract.cfm?URI=ol-34-9-1363>.
- [31] M. T. Cicerone, K. A. Aamer, Y. J. Lee, and E. Vartiainen, *Journal Of Raman Spectroscopy* **43**, 637 (2012).
- [32] L. Lepetit, G. Chériaux, and M. Joffre, *J. Opt. Soc. Am. B* **12**, 2467 (1995), URL <http://josab.osa.org/abstract.cfm?URI=josab-12-12-2467>.
- [33] W. Langbein, I. Rocha-Mendoza, and P. Borri, *Applied Physics Letters* **95**, 081109 (2009).
- [34] D. A. Kleinman, *Phys. Rev.* **126**, 1977 (1962), URL <http://link.aps.org/doi/10.1103/PhysRev.126.1977>.
- [35] D. Gachet, N. Sandeau, and H. Rigneault, *Journal Of The European Optical Society-Rapid Publications* **1**, 06013 (2006).
- [36] J. K. Wilmschurst and H. J. Bernstein, *Canadian Journal of Chemistry* **35**, 911 (1957), <http://www.nrcresearchpress.com/doi/pdf/10.1139/v57-123>, URL <http://www.nrcresearchpress.com/doi/abs/10.1139/v57-123>.
- [37] M. A. Yuratich and D. C. Hanna, *Molecular Physics* **33**,

671 (1977).

[38] See Supplemental Material at [URL will be inserted by publisher] for derivation of the SIP-CARS amplitude for arbitrary ellipticities.

[39] See Supplemental Material at [URL will be inserted by publisher] for comparison of the full SIP-CARS and spontaneous Raman spectra.